

Matter and J/ψ Suppression

Jörg Hüfner^{a,b}, Boris Z. Kopeliovich^{b,c} and Alberto Polleri^a

^a *Institut für Theoretische Physik der Universität, Philosophenweg 19, D-69120 Heidelberg, Germany.*

^b *Max Planck Institut für Kernphysik, Postfach 103980, D-69029 Heidelberg, Germany.*

^c *Joint Institute for Nuclear Research, Dubna, 141980 Moscow Region, Russia.*

Abstract

In high energy nuclear collisions, the conventional Glauber model is commonly used to evaluate the contribution to J/ψ suppression originating from the inelastic interaction with colorless bound nucleons. This requires an effective value for the J/ψ -nucleon absorption cross section which is larger than theoretically expected. On the other hand, multiple nucleon-nucleon collisions mediated by color exchange interactions, excite their color degrees of freedom. We investigate the importance of this effect and find that these excited states provide a larger cross section for J/ψ absorption. We conclude that the related corrections are important to explain the effective value extrapolated from experiment.

1 Introduction

The origin of the anomalous behavior of the J/ψ production cross section, as measured in Pb+Pb collisions at the CERN-SPS is still debated and several competing interpretations have so far been proposed. For a review on the subject see [1, 2].

In the early stage of a nucleus-nucleus (AB) collision, the production mechanism of a charmonium is controlled by four length scales. They are the coherence length $l_c \leq 2 E_{J/\psi}/m_{J/\psi}^2$, the formation length $l_f \simeq 2 E_{J/\psi}/(m_{\psi'}^2 - m_{J/\psi}^2)$, the mean interparticle distance $\lambda \simeq 2$ fm in a nucleus and the mean nuclear size $R_{A,B} \simeq 5 - 6$ fm for large nuclei. Their interplay is crucial for the correct theoretical formulation of the problem and understanding the nature of early stage suppression. In the kinematic regime of the NA38/50 experiment at the CERN-SPS, which detects charmonia with $p_{lab} = 50$ GeV, one has $l_c \leq 2$ fm and $l_f \simeq 5$ fm. Therefore, since l_c is shorter than the mean nucleon separation,

one can assume that the colorless $c\bar{c}$ wave packet is produced in elementary nucleon-nucleon (NN) interactions. On the other hand, the formation length is of the order of the nuclear size and the charmonium takes a finite path in the nucleus before being fully formed. The effect of these length scales on hadronic processes in a nuclear environment has been extensively studied [3, 4, 5, 6] and experimentally observed in electroproduction of ρ mesons off nuclei [7]. Nevertheless, J/ψ suppression is mostly treated within the Glauber model, with a constant effective cross section for absorption on bound, non-interacting nucleons. Only recently [5, 8], the effect caused by the formation length was taken into account in the present context. Notice that while studying the SPS data it is justified to neglect the contribution of the coherence length, for RHIC data it will not be so, being $l_f \gg l_c \gg R_{A,B}$, and a new regime will open up. For the present discussion on SPS data, the relevant scales for J/ψ absorption are l_f and $R_{A,B}$, governing the suppression at the early stage.

After the early stage, governed by NN collisions, an excited medium with high energy density is left behind. It is not yet clear how to describe it, but several points of view have been put forward. It is possible that the properties of the excited medium are similar to those of a plasma of de-confined quarks and gluons. This was indeed the original motivation for making J/ψ suppression so interesting [9]. It has been argued that such a plasma is very opaque to charmonium, therefore preventing its final observation as a bound state [10, 11]. In the last stage of the reaction, part of the large number of produced hadrons, the so called co-movers, is possibly also responsible for suppression [12, 13, 14].

The present work intends to study the early stage nuclear absorption of J/ψ . It is common practice to approach the problem assigning a constant value to the J/ψ -nucleon absorption cross section. This quantity is then considered as an effective parameter, fitted in order to reproduce the production data in proton-nucleus (pA) collisions. Our goal is to improve the understanding of the physical phenomena behind early stage absorption, neglecting for the time being other possible effects and therefore not necessarily being able to describe of the full set of available data.

Following a known interpretation of the dynamics of NN collisions, we ascribe the main contribution to the inelastic cross section to color exchange processes. This assumption is well supported by high-energy hadron collision data, showing a plateau in the rapidity distribution of produced particles and indicating that the real part of the scattering amplitude is small with respect to the imaginary one.

Via color exchange, the 3-quark systems constituting the colliding nucleons become color octet states. It was already mentioned in [15] that each colliding system is colored, although the possible effects of this were neglected for simplicity. Color exchange may also be accompanied by gluon radiation. While the contribution of radiated gluons to J/ψ absorption was treated in [15, 16], here we focus on the first part. Having realized that color-singlet nucleons are found in color octet states after an elementary collision, one can expect that repeated scatterings lead to multiple color exchanges. One therefore has the possibility to excite the color degrees of freedom of the 3-quark system also to the decuplet state. Higher color representations can be obtained when radiated gluons are also present, but here we restrict our study on the color dynamics of the constituent quarks of a nucleon.

In the next section we calculate the cross sections for the interaction of charmonium with a colored nucleon. We find an increase of 35 % when the 3-quark system is in octet state, with respect to the case when it is a color singlet, while with the decuplet the increase is of 70 %. We analyze and discuss in detail pA collisions in the third section. Finally, we consider the AB case: the effect of multiple scattering is studied and then applied to calculate integrated production cross sections. We find an increased absorption, although the experimental suppression in the Pb+Pb cross section cannot be explained by the present treatment. The concluding section critically examines the results and gives an outlook on possible further improvements. Throughout the paper we indicate with Ψ the effective charmonium state, composed by a mixture of J/ψ , ψ' and χ .

2 Interaction of Charmonium with Colored Nucleons

The main feature we want to stress is the property of the color exchange interaction for the high energy collision amplitude. Repeated collisions allow a nucleon to be in any color SU(3) representation $\mathbf{3} \otimes \mathbf{3} \otimes \mathbf{3} = \mathbf{1} \oplus \mathbf{8}_A \oplus \mathbf{8}_S \oplus \mathbf{10}$. To calculate the value of the inelastic cross section for Ψ on a nucleon which has undergone multiple scattering, we use the two-gluon exchange model of Low and Nussinov [17, 18]. Although oversimplified, the model incorporates important properties of high-energy hadronic cross sections such as (approximate) energy independence and scaling of the cross sections according to the mean square radius of hadrons. One can write at once the absorption cross section, making use of the optical theorem, relating it to the forward elastic amplitude. This is convenient, since the

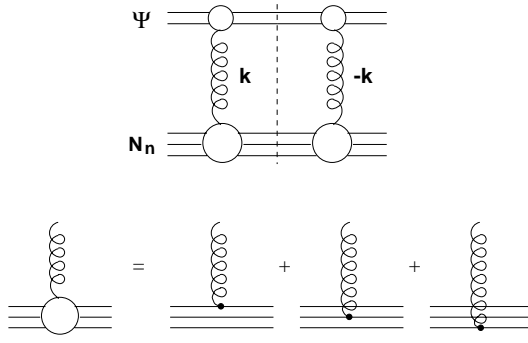


Figure 1: Top: Diagram illustrating the meson-nucleon elastic amplitude. The dashed line indicates the unitarity cut. Bottom: Vertex Γ between a gluon and the three-quark system of a nucleon.

latter amplitude, in the two gluon exchange approximation, is purely imaginary. One obtains

$$\sigma_{\Psi N}^{abs} = \int d^2 \vec{r} \langle \Psi, N_n | \left[\sum_{i,j} V(\vec{b} + \vec{x}_i - \vec{y}_j) \right]^2 | \Psi, N_n \rangle. \quad (1)$$

It is a diagonal matrix element between a product state of charmonium Ψ and a nucleon N_n in its color representation n . The variable \vec{b} is the impact parameter between the scattering hadrons. The transverse coordinates $\vec{y}_{1,2,3}$ refer the quarks in the nucleon, while $\vec{x}_{1,2}$ are those of Ψ . In the square brackets one has the transverse part of the one-gluon exchange potential. We define its Fourier transform as

$$V(\vec{z}) = \int \frac{d^2 \vec{k}}{(2\pi)^2} \frac{1}{2} g_s \lambda_{(i)}^a \frac{\exp(i \vec{k} \cdot \vec{z})}{k^2 + \mu^2} \frac{1}{2} g_s \lambda_{(j)}^a, \quad (2)$$

where g_s is the quark-gluon QCD coupling and μ is an effective gluon mass, introduced to incorporate confinement. The index in parenthesis labeling the Gell-Mann matrices indicates to which quark the vertex is attached. Light-cone wave functions are used for Ψ and N_n in the expectation value (1). For the nucleon, we assume that the transverse positions of the quarks in the nucleon are frozen during the early stage of the collision, and therefore use the same spatial distribution both for singlet and colored states.

Inserting in eq. (1) the expression for the gluon potential given in eq. (2) and performing the impact parameter integration, one arrives at the relation

$$\begin{aligned} \sigma_{\Psi N_n}^{abs} = & \int d^2 \vec{k} \frac{1}{(k^2 + \mu^2)^2} \langle \Psi | 1 - \exp(i \vec{k} \cdot \vec{x}_{12}) | \Psi \rangle \\ & \times \langle N_n | \Gamma^a(k) \Gamma^{\dagger a}(k) | N_n \rangle, \end{aligned} \quad (3)$$

illustrated in the top part of FIG. 1. The first factor in the integrand is the squared gluon propagator, the second contains the phase shift due to the momentum transfer \vec{k} and is responsible, by the way, for color transparency, while the last factor is the interesting part of the present calculation. It is the product of two vertices between three quarks and a gluon, averaged with the wave function of the colored nucleon. The vertex, illustrated in the bottom part of FIG. 1, is

$$\begin{aligned}\Gamma^a(k) = & \frac{16}{3}\alpha_s \left[(\lambda_{(1)}^a)_{i'}^i \delta_{j'}^j \delta_{k'}^k \exp(i \vec{k} \vec{y}_1) \right. \\ & + \delta_{i'}^i (\lambda_{(2)}^a)_{j'}^j \delta_{k'}^k \exp(i \vec{k} \vec{y}_2) \\ & \left. + \delta_{i'}^i \delta_{j'}^j (\lambda_{(3)}^a)_{k'}^k \exp(i \vec{k} \vec{y}_3) \right].\end{aligned}\quad (4)$$

In order to average the product of the two vertices, one needs to specify the structure of the nucleon wave function. The color part of the wave function is the relevant one, while the spatial part is chosen to be equal for all color multiplets. We (anti)symmetrize quarks 1 and 2 in order to construct the mixed-symmetry octets, therefore use

$$\phi_{ijk}^n = \begin{cases} \frac{1}{\sqrt{6}} \epsilon_{ijk} & \{\mathbf{1}\}, \\ \frac{1}{\sqrt{2}} \left[\delta_k^r \epsilon_{ijs} - \frac{1}{3} \delta_s^r \epsilon_{ijk} \right] & \{\mathbf{8}_A\}, \\ \frac{1}{\sqrt{6}} \left[\delta_i^r \epsilon_{jks} + \delta_j^r \epsilon_{iks} \right] & \{\mathbf{8}_S\}, \\ \frac{1}{6} \left[\delta_i^r \delta_j^s \delta_k^t + \text{perm. of } r, s, t \right] & \{\mathbf{10}\}. \end{cases}\quad (5)$$

Because of the $SU(3)$ structure, the different color multiplets have different number of indices. For simplicity, we label with n the different multiplets. The factor given by the angular brackets in eq. (3) can now be evaluated. It involves the contraction of all the indices, leading to

$$\langle N_n | \Gamma^a \Gamma^{\dagger a} | N_n \rangle = \langle N | \sum_{i < j} 1 - c_n \exp(i \vec{k} \vec{y}_{ij}) | N \rangle. \quad (6)$$

The effect of having different color states is all contained in the coefficients c_n , listed in the second column of TABLE 1. It turns out that matrix elements with $n = \mathbf{8}_A, \mathbf{8}_S$ are identical. The values of c_n found, for $n = \mathbf{8}, \mathbf{10}$, lead to larger absorption cross sections as compared to the singlet case. To see this it is useful to define the two-quark form factor $F_N^{2q}(k^2) = \langle N | \exp(i \vec{k} \vec{x}_{ij}) | N \rangle$ for the nucleon. Since, within our approximation, the latter does not depend on the colour multiplet, we drop the label n . Then we can rewrite eq. (3) as

$$\sigma_{\Psi N_n}^{abs} = \langle \Psi | \sigma_n(r) | \Psi \rangle, \quad (7)$$

where the function in the brackets is

$$\begin{aligned} \sigma_n(r) = & \frac{16}{3} \alpha_s^2 \int d^2 \vec{k} \frac{1}{(k^2 + \mu^2)^2} [1 - \exp(i \vec{k} \cdot \vec{r})] \\ & \times [1 - c_n F_N^{2q}(k^2)], \end{aligned} \quad (8)$$

exhibiting a similar structure to that of the usual dipole-nucleon cross section, but with the important difference carried by the coefficients c_n . Notice that with $c_n \neq 1$ and $\mu = 0$ the integral in eq. (8) is infrared divergent. Therefore, the cut-off μ , of the order of the inverse confinement radius, is important. With $\mu \neq 0$ it holds that $\sigma_n(r) \rightarrow 0$ for $r \rightarrow 0$, so that one still preserves color transparency, even with a colored nucleon. This is indeed a property of the singlet meson. In our work we are not primarily interested in the absolute values of $\sigma_{\Psi N_n}^{abs}$ but rather on its dependence on the color state n with respect to the singlet value. Yet we estimated the absolute values choosing $\alpha_s = 0.6$ and $\mu = 140$ MeV. Within a harmonic oscillator model of the nucleon, one finds that $F_N^{2q}(k^2) = F_N^{em}(3k^2)$, the electromagnetic form factor. We assume that this property is general and take the dipole form

$$F_N^{em}(Q^2) = \left(\frac{\tilde{\lambda}^2}{\tilde{\lambda}^2 + Q^2} \right)^2 \underset{Q^2 \rightarrow 0}{\simeq} 1 - \frac{1}{6} Q^2 R_p^2, \quad (9)$$

where the last approximate equality allows to fix the parameter $\tilde{\lambda}^2 = 12/R_p^2$, with $R_p = 0.8$ fm. For convenience we rescale $\tilde{\lambda}^2 = 3\lambda^2$, so that $\lambda = 2/R_p$. With the above definitions, the generalized dipole-nucleon cross section can be computed analytically in terms of modified Bessel functions K_0 and K_1 , with the result

$$\begin{aligned} \sigma_n(r) = & \frac{16\pi\alpha_s^2}{3\lambda^2} \left\{ \frac{1 - D_2^n(\xi)}{\xi^2} H(\mu r) - D_2^n(\xi) H(\lambda r) \right. \\ & \left. - D_3^n(\xi) [\log(\xi) + K_0(\mu r) - K_0(\lambda r)] \right\}, \end{aligned} \quad (10)$$

being $D_2^n(\xi) = c_n/(1 - \xi^2)^2$, $D_3^n(\xi) = 4c_n/(1 - \xi^2)^3$, $\xi = \mu/\lambda$ and $H(r) = 1 - zK_1(r)$. The results of the calculation, illustrated in FIG. 2, shows the modified dipole-nucleon cross section for the three

Table 1: Results of the calculation of the meson-colored nucleon cross sections.

Multiplet	$\{n\}$	c_n	$\sigma_{\psi N_n}$ [mb]	δ_n
Singlet	$\{\mathbf{1}\}$	1	5.8	1.0
Octet	$\{\mathbf{8}\}$	$-1/4$	7.8	1.35
Decuplet	$\{\mathbf{10}\}$	$1/2$	9.9	1.7

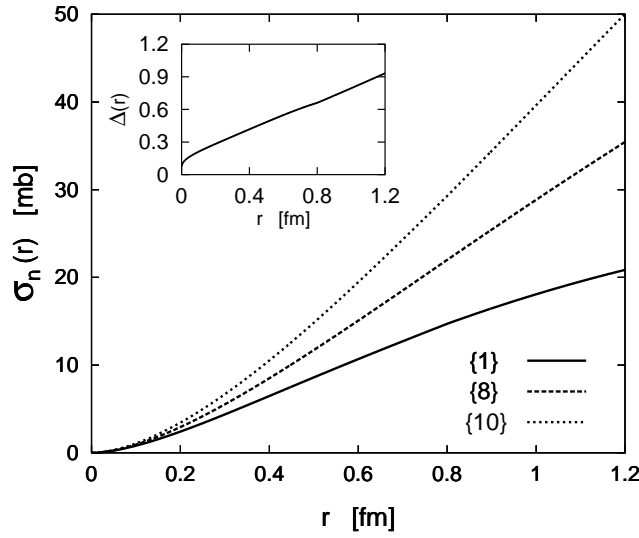


Figure 2: Dipole cross section for different color states as a function of the quark separation r . Box: The quantity $\Delta(r)$ which governs the dependence on color.

color states of the nucleon. It largely increases when the dipole scatters off a colored object. One can get more insight in the effect of the different color states rewriting eq. (8) in the form

$$\sigma_n(r) = \sigma(r) [1 + (1 - c_n) \Delta(r)] , \quad (11)$$

where $\sigma(r)$ is the usual dipole cross section on a color singlet nucleon and the function $\Delta(r)$ is found to vary appreciably with r . Its functional dependence is given in the small box in Fig. 2. To calculate the inelastic cross section according to eq. (7), we must average σ_n with the meson wave function. Therefore, the dependence of Δ on r shows that the effect of having colored nucleons is stronger for larger size mesons. Recent calculations [19], based on realistic phenomenology for the dipole cross section and charmonium wave function, gave values for cross sections of various charmonia on a nucleon. At center of mass energy $\sqrt{s} = 10$ GeV, it was found that $\sigma_{J/\psi N} = 3.6$ mb, $\sigma_{\psi' N} = 12.2$ mb and $\sigma_{\chi N} = 9.1$ mb. With a composition of Ψ of 52-60% due to J/ψ , 8-10% due to ψ' and 32-40% due to χ , a weighted value of 5.8 mb was obtained. In the present case we evaluate $\sigma_{\Psi N_n}^{abs}$ with a Gaussian wave function having root mean square transverse separation $\langle r^2 \rangle^{1/2} = 0.25$ fm, in order to account for the different states (J/ψ , ψ' , χ) implicitly included in Ψ and therefore adjust the singlet cross section to the quoted 5.8 mb. The values found are given in the third column of TABLE 1. In order to minimize the model dependence, we factored out from the colored cross sections the amount

corresponding to the singlet case, therefore writing $\sigma_{\psi N_n}^{abs} = \sigma_{\psi N}^{abs} \delta_n$. The values for δ_n are given in the last column of TABLE 1. They constitute the important result of this calculation, showing that Ψ scatters with an color octet nucleon with a 35 % larger cross section with respect to a singlet nucleon, while with the decuplet the increase is even of 70 %. The large values found now require a careful analysis to establish the validity of this newly proposed absorption mechanism.

3 Analysis of proton-nucleus data: is the color mechanism already at work ?

Since the absorption pattern observed in pA collisions is usually considered to be the baseline for the AB case, it is necessary to examine it in some detail in the light of the possibility of a color mechanism for charmonium absorption.

Consider the illustration given in FIG 3. There one can see the longitudinal and transverse geometry of the collision between a proton and the row of target nucleons with which it collides. On the left hand side one sees the projectile P which collides with the target nucleon T_1 , producing a would be Ψ meson. Successively the projectile interacts with the target nucleon T_2 which, then, collides with the Ψ meson. According to our initial argument, each nucleon-nucleon collision leaves the nucleons in a color octet state. As illustrated on the right hand picture, since Ψ is produced by P, it is overlapping with it. If then the charmonium is struck by T_2 , P and T_2 must also overlap, indicating that they have previously interacted. Therefore, in a pA collision all the nucleons with which Ψ has an interaction are color octets. This means that the effective absorption cross section normally used in Glauber model calculations in order to reproduce pA data, should be the cross section with a color octet nucleon. On the other hand, another simple geometrical argument shows that this might not be the full truth. In fact, in order to claim that Ψ interacts with a colored nucleon, the charmonium state itself is required to be well separated from the parent projectile 3-quark system, preceeding Ψ in propagation through the nucleus. This takes a finite time, since the charmonium is produced inside the projectile and has a smaller velocity. In the rest frame of the nucleus, the difference in velocities between Ψ and the parent 3-quark system is $\Delta v \simeq m_\Psi^2/2E_\Psi^2 - m_p^2/2E_p^2$, being $v = \sqrt{1 - m^2/E^2} \simeq 1 - m^2/2E^2$. Therefore, one requires a finite length $L = R_p/\Delta v$, with $R_p = R_p^{(0)}/\gamma_p$, in order to have the charmonium separated from the projectile. In the following we focus on the kinematics of the NA38/50 experiments at the

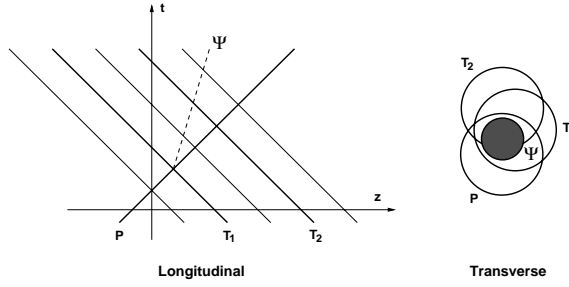


Figure 3: Left: Longitudinal space-time representation of charmonium production in a pA collision, in the c.m. frame of a NN collision. Right: Illustration of the overlap between projectile (P), parent target (T_1) and nucleon with which Ψ scatters inelastically (T_2).

CERN-SPS, for charmonia with laboratory momentum $p_\Psi = 50$ GeV and consider projectile protons with at least $E_p = 200$ GeV. Then, since $\gamma_p = E_p/m_p$, taking $R_p^{(0)} = 0.8$ fm we obtain $L = 2$ fm. The physical meaning of L is the following: After its creation, the charmonium has to travel a length L (in the target rest frame) before one can safely assume that the next interaction occurs with a colored nucleon. Since the mean length which Ψ travels inside a nucleus is $2/3 R_A$, the retardation length L reduces the effect of colored nucleons considerably. It destroys it in light nuclei with $A \leq 50$, and it reduces it to about 50% in heavy nuclei.

Now, before we analyze the data for charmonium production in pA collisions, we discuss the importance of charmonium formation time, introduced in a quantum-mechanical way in [3, 5]. Within a simplified version of a two-channel model [8], the ΨN absorption cross section evolves in the eigentime τ of Ψ as

$$\sigma_{\Psi N}^{abs}(\tau) = \sigma_{\Psi N}^{in} + (\sigma^{(0)} - \sigma_{\Psi N}^{in}) \cos(\tau/\tau_f), \quad (12)$$

where $\tau_f = (m_{\psi'} - m_{J\psi})^{-1} = 0.3$ fm is the charmonium formation time, $\sigma_{\Psi N}^{in}$ is the inelastic ΨN cross section and $\sigma^{(0)} = \sigma_{\Psi N}^{abs}(\tau = 0)$ is the cross section of the so called “pre-meson” on a nucleon. As mentioned in the last section, calculations give $\sigma_{\Psi N}^{in} = 5.8$ mb [19]. Unfortunately $\sigma^{(0)}$ has not yet been calculated. We therefore use the value 2.7 mb from [8].

Making use of eq. (12), one can then write the expression for Ψ production in pA collisions, normalized to one nucleon, as

$$\sigma_{\Psi}^{pA} = \sigma_{\Psi}^{NN} \frac{1}{A} \int d^2\vec{b} dz \quad (13)$$

$$\times \left[1 - \int_z^{+\infty} dz' \sigma_{\Psi N}^{abs} \left(\frac{z'-z}{\gamma_{\Psi}} \right) \rho_A(z, \vec{b}) / A \right]^{A-1}.$$

We now want to compare this expression with the conventional one obtained in the Glauber model, containing only an effective absorption cross section, therefore making the replacement $\sigma_{\Psi N}^{abs}(\tau) \rightarrow \sigma_{\Psi N}^{eff}$. In this way one can perform the z -integration and obtain the well known formula

$$\sigma_{\Psi}^{pA} = \sigma_{\Psi}^{NN} \int d^2\vec{b} \frac{1 - \left[1 - \sigma_{\Psi N}^{eff} T_A(\vec{b}) / A \right]^A}{\sigma_{\Psi N}^{eff} A}, \quad (14)$$

being $T_A(\vec{b})$ the nuclear thickness function.

For $A = 208$ and $p_{\Psi} = 50$ GeV, using a realistic profile for Pb [20] and forcing the two expressions in eqs. (13) and (14) to be equal, we obtain $\sigma_{\Psi N}^{eff} = 3.8$ mb. This number has to be interpreted as the value of the effective absorption cross section of Ψ on a color singlet nucleon, including formation time effects. To obtain the corresponding value for the case when Ψ scatters on a color octet nucleon, according to the result of the previous section we have to enhance the singlet result by 35%, obtaining 5.1 mb. The values of $\sigma_{\Psi N}^{eff} = 3.8$ mb and 5.1 mb are indicated as full lines in FIG. 4. Because of a possible retardation of the color mechanism, we expect the experimental values to lie between these two lines.

We have then re-analyzed the existing data taken by 3 fixed target experiments: NA3 at CERN [21], which measured the ratio of Ψ production cross sections between Pt and H₂ for 200 GeV projectile protons; NA38/51 [22] at CERN, which measured the cross section for different targets (H₂, D₂, C, Al, Cu, W) struck by 450 GeV protons; E866 at FERMILAB [23], which measured the ratio of cross sections between W and Be for 800 GeV protons. In order to remove the effects on absorption due to different Ψ momenta, we impose the same kinematic conditions, considering Ψ 's of 50 GeV momentum in the laboratory frame, corresponding to $x_F = 0.15, 0.01, -0.04$ respectively, for the three experiments. We then assume that the absorption mechanism is parameterized by the effective cross section $\sigma_{\Psi N}^{eff}$, appearing in the Glauber model expression given in eq. (14). The ratio of cross sections is defined as

$$R_{A/B} = \sigma_{\Psi}^{pA} / \sigma_{\Psi}^{pB}. \quad (15)$$

Therefore, while the pA cross section depends on the two parameters σ_{Ψ}^{NN} and $\sigma_{\Psi N}^{eff}$, the ratio depends only on the latter. We made three separate fits using the MINUIT package from CERNLIB, including

quoted statistical and systematic errors for the various cross sections and ratios. We extract the effective absorption cross section by minimizing χ^2 . The result of these fits is presented in the second column of TABLE 2. The average is obtained, using the weights $w_i = 1/\delta\sigma_i^2$, as $\bar{\sigma} = \sum_i w_i \sigma_i / \sum_i w_i$, while the error is $\delta\sigma = (\sum_i w_i)^{-1/2}$. The values extracted from experiment are represented as open points in FIG. 4. The mean value of 3.5 ± 0.6 mb seems to favor the singlet mechanism, for which a cross section of 3.8 mb is theoretically expected.

On the other hand, the assumption that Ψ is produced on a bound nucleon with the same cross section as on a free one, used in eq. (14), can be an oversimplification of the physics under study. We know that in a nuclear environment parton distributions are substantially modified [24, 25, 26]. In particular, the gluon distribution in nuclei exhibits anti-shadowing effects at $x_{Bj} \simeq 0.1$, *i.e.* the gluon distribution $g_A(x_2, Q^2)$ in a nucleus is larger than the one in a nucleon $g(x_2, Q^2)$. We expect that charmonium production on a nucleus is enhanced by a factor $R_A^g(x_2, Q^2) = g_A(x_2, Q^2)/g(x_2, Q^2)$. We estimate these effects by rescaling the Ψ cross section with the A-dependent correction $R_A^g = 0.032 \log(A) + 1.006$, extracted from [26]. For a heavy nucleus this amounts to an enhancement of the production cross section by a factor of nearly 1.2, therefore requiring a larger $\sigma_{\Psi N}^{eff}$. We fit the data once more, obtaining the results listed in the third column of TABLE 2. One sees that the new average value of 5.7 ± 0.6 mb now seems to favor the octet mechanism, for which we estimated a value of 5.1 mb. The results of the fits, together with the theoretical expectations, are all plotted in FIG. 4, where the full points are the result of accounting for anti-shadowing. One observes that the situation is, in all, quite uncertain.

The above analysis is based on the assumption that there is no dependence of nuclear effects

Table 2: Results of the fits to pA data for the various experiments considered. See text for details.

Experiments $p_\psi = 50$ GeV	$\sigma_{\psi N}^{abs}$ [mb]	
	Glauber fit	Gluon corr.
NA3	4.5 ± 1.7	7.3 ± 1.9
NA38/51	7.1 ± 1.6	10 ± 1.8
E866	2.7 ± 0.7	4.7 ± 0.7
Averages	3.5 ± 0.6	5.7 ± 0.6
Theory	3.8 {1}	5.1 {8}

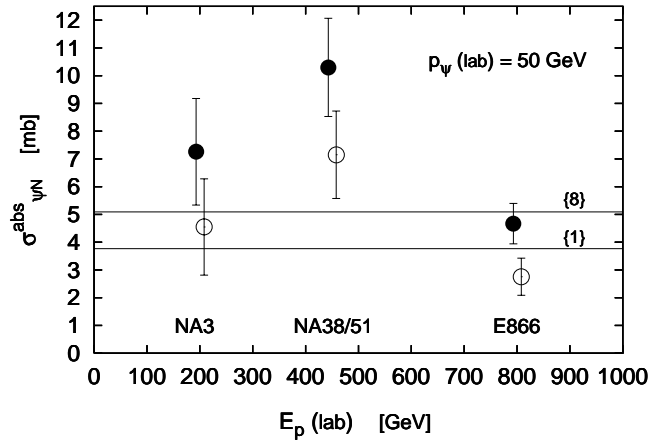


Figure 4: Results of the fits to pA data for the various experiments considered. Open dots refer to the Glauber model fit while full dots account for gluon anti-shadowing corrections. The horizontal lines indicate the theoretical expectations for the singlet and octet absorption mechanisms, respectively.

on the proton energy, is the charmonium energy is the same in all experiments. This is justified in many phenomena, e.g. the coherence time effect [4]. However, there might still be some dependence on the proton energy. According to [27], energy loss of the projectile gluon in the nuclear medium substantially reduces the production rate of charmonia at large x_F and is still rather important at small x_F . In order to compensate for energy loss, the gluon distribution must be evaluated at a higher value of x_1 , therefore suppressing Ψ production. This will in turn reduce the final state absorption on nucleons in a fit to the data. To account for this effect, already observed in Drell-Yan data [28], further study, which goes beyond the scope of this paper, is required.

To summarize, the data seem to suggest that Ψ is absorbed by colored nucleons in pA collisions. The picture is though not yet conclusive due to the large experimental errors. Nevertheless, we follow our theoretical prediction and examine the potential role of the color mechanism in the more complex case of AB collisions.

4 Color dynamics in nucleus-nucleus collisions

Preparing the ground for the forthcoming discussion, it is useful to recall the conventional expression within the Glauber model for the Ψ production cross section at impact parameter \vec{b} . Generalizing

eq. (13), to the case of AB collisions, one simply obtains

$$\begin{aligned}
\frac{d^2\sigma_{\Psi}^{AB}}{d^2\vec{b}}(\vec{b}) &= \int d^2\vec{b}_A dz_A d^2\vec{b}_B dz_B \delta^2(\vec{b}_A + \vec{b}_B - \vec{b}) \sigma_{\Psi}^{NN} \\
&\times \rho_A(z_A, \vec{b}_A) \left[1 - \sigma_{\Psi N}^{abs} T_A(z_A, \vec{b}_A)/A\right]^{A-1} \\
&\times \rho_B(z_B, \vec{b}_B) \left[1 - \sigma_{\Psi N}^{abs} T_B(z_B, \vec{b}_B)/B\right]^{B-1} \\
&\times S_{F.S.I.}(z_A, z_B, \vec{b}_A, \vec{b}_B),
\end{aligned} \tag{16}$$

which describes the collision of two rows at impact parameters \vec{b}_A and \vec{b}_B , overlapping due to the δ -function. ρ_A and ρ_B are the nuclear densities while

$$\begin{aligned}
T_A(z_A, \vec{b}_A) &= \int_{-\infty}^{z_A} dz'_A \rho_A(z'_A, \vec{b}_A) \quad \text{and} \\
T_B(z_B, \vec{b}_B) &= \int_{z_B}^{+\infty} dz'_B \rho_B(z'_B, \vec{b}_B)
\end{aligned}$$

are the thickness functions. The last factor $S_{F.S.I.}(z_A, z_B, \vec{b}_A, \vec{b}_B)$ represent the probability of survival due to any additional “anomalous” suppression factor which goes beyond conventional nuclear effects, that is final state interactions with the produced matter (QGP, hadron gas, etc.). Here we are not primarily interested in these contributions, therefore set $S_{F.S.I.} = 1$. On the other hand, we focus on the reinterpretation of the terms describing nuclear effects discussing, in the next two subsections, color exchange in the context of multiple scattering, then applying the obtained results to the calculation of Ψ production in AB collisions.

1 Multiple color exchange in a nucleus

Having completed the computation of the Ψ cross sections with colored nucleons, we need to look at how these color objects develop in a collision between nuclei. Consider a nucleon of one of the nuclei colliding with a row of nucleons of the other nucleus. It undergoes multiple scattering, with repeated color exchanges. Keeping the projectile quark coordinates $\vec{y}_{1,2,3}$ frozen, according to the high-energy approximation, it is possible to calculate the probability $\mathcal{P}_n(\{\vec{y}_j\}, z, \vec{b})$ for a nucleon in color state $n = \mathbf{1, 8, 10}$ after having traveled through the row up to z at impact parameter \vec{b} . This can be done in a very elegant way, by solving an evolution equation for the color density matrix of the 3-quark system. The problem has been considered some time ago with the general aim of studying the color

exchange interaction in the nuclear environment. A detailed calculation [29] shows that

$$\mathcal{P}_n = \frac{1}{27} \times \begin{cases} 1 + 20 \mathcal{F} + 2 \mathcal{G} & \{\mathbf{1}\} \\ 16 - 40 \mathcal{F} + 8 \mathcal{G} & \{\mathbf{8}\} \\ 10 + 20 \mathcal{F} - 10 \mathcal{G} & \{\mathbf{10}\} \end{cases}, \quad (17)$$

where

$$\mathcal{F}(\{\vec{y}_j\}, z, \vec{b}) = \exp \left[-\frac{9}{16} \sum_{i < j} \sigma(y_{ij}) T(z, \vec{b}) \right] \quad (18)$$

and

$$\mathcal{G}(\{\vec{y}_j\}, z, \vec{b}) = \sum_{i < j} \exp \left[-\frac{9}{8} \sigma(y_{ij}) T(z, \vec{b}) \right]. \quad (19)$$

The coefficients \mathcal{F} and \mathcal{G} are expressed in terms of the standard dipole cross section $\sigma(y_{ij})$, appearing in eq. (11), which one can construct by pairing two of the three quarks in a nucleon. Their arguments are the differences of quark coordinates $\vec{y}_{ij} = \vec{y}_i - \vec{y}_j$. The thickness function $T(z, \vec{b})$ can be taken as that of nucleus A or B , depending on which nucleus one is considering. We can average the probabilities with spatial nucleon wave functions as

$$P_n(z, \vec{b}) = \langle N | \mathcal{P}_n(\{\vec{y}_j\}, z, \vec{b}) | N \rangle, \quad (20)$$

therefore integrating over internal quark coordinates. Due to the structure of eq. (17), the averaging procedure expressed by eq. (20) is transferred to an average of \mathcal{F} and \mathcal{G} . In analogy to the definition of $P_n(z, \vec{b})$, we will define also the functions $F(z, \vec{b})$ and $G(z, \vec{b})$. This average can in principle be exactly evaluated, although in practice one needs to know the correct form of the dipole cross section and of the spatial distribution of the three quarks in a nucleon. We therefore choose to average the exponents appearing in eqs. (18) and (19), instead of the full exponentials, *i.e.* evaluating $\exp(-\langle N | X | N \rangle)$ instead of $\langle N | \exp(-X) | N \rangle$ for a given X . This corresponds to neglecting inelastic shadowing corrections which, according to [30, 31], are small. Due to rotational symmetry one has $\langle \sigma(y_{ij}) \rangle = 2/3 \sigma_{NN}^{in}$ for all i, j . We took the value $\sigma_{NN}^{in} = 30$ mb. In this way one obtains

$$P_n(z, \vec{b}) = \frac{1}{27} \times \begin{cases} 1 + 20 F(z, \vec{b}) + 6 G(z, \vec{b}) & \{\mathbf{1}\} \\ 16 - 40 F(z, \vec{b}) + 24 G(z, \vec{b}) & \{\mathbf{8}\} \\ 10 + 20 F(z, \vec{b}) - 30 G(z, \vec{b}) & \{\mathbf{10}\} \end{cases}, \quad (21)$$

where

$$F(z, \vec{b}) = \exp \left[-\frac{9}{8} \sigma_{NN}^{in} T(z, \vec{b}) \right] \quad (22)$$

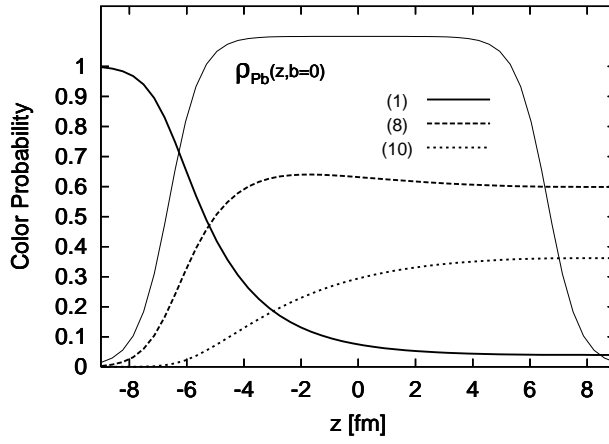


Figure 5: Evolution of the color probabilities P_1 , P_8 , P_{10} , along z and with $\vec{b} = 0$. Also shown is the profile $\rho_{\text{Pb}}(z, \vec{b} = 0)$ of a Pb nucleus.

and

$$G(z, \vec{b}) = \exp \left[-\frac{3}{4} \sigma_{NN}^{\text{in}} T(z, \vec{b}) \right]. \quad (23)$$

One notices several properties of the probabilities. First of all, the limit $T \rightarrow 0$ implies $F, G \rightarrow 1$. This means that $P_1 \rightarrow 1$ and $P_8, P_{10} \rightarrow 0$. In other words the nucleon, before entering the nucleus, is in singlet state as it should be. Moreover, $P_1 + P_8 + P_{10} = 1$ for any T , therefore probability is always conserved. Finally, if the nucleus is large enough one has $T \gg 1$ and $F, G \ll 1$. This implies that if sufficient scatterings have taken place, the color probabilities reach the statistical limit, given by the first coefficients of eqs. (21). In other words, the 3-quark system becomes unpolarized in color after many collisions. Out of 27 states, one is the singlet, 16 are in the two octets and 10 are in the decuplet. The z -dependence of the color probabilities is illustrated in FIG. 5, together with the longitudinal profile $\rho_{\text{Pb}}(z, \vec{b})$ of a Pb nucleus. Soon after the nucleon has penetrated the nuclear profile, a process that involves ~ 4 fm corresponding to 2 nucleon mean free paths, the statistical limit is essentially reached in which about $16/27 \simeq 2/3$ of the nucleons are in octet state while $10/27 \simeq 1/3$ are in decuplet. The amount of singlet is negligible.

With the calculated probabilities P_n and the previously evaluated color cross sections $\sigma_{\Psi N_n}^{\text{abs}}$, we can now construct the cross section for Ψ when it scatters with a nucleon, taking into account all its

color states. We obtain

$$\sigma_{\Psi N}^{abs}(z, \vec{b}) = \sum_n \sigma_{\Psi N_n}^{abs} P_n(z, \vec{b}). \quad (24)$$

As obvious from FIG. 5, the projectile nucleon which collides with several target nucleons quickly reaches a “color equilibrium”. Using the values for δ_n given in TABLE 1, that is 1.35 for the octet cross section and 1.7 for the decuplet one, the effective absorption cross section of Ψ on a nucleon, within a nucleus-nucleus collision, becomes

$$\begin{aligned} \sigma_{\psi N}^{abs}(z, \vec{b}) &\xrightarrow[\vec{b}=0]{z \rightarrow \infty} \left[\frac{1}{27} + \frac{16}{27} \times 1.35 + \frac{10}{27} \times 1.7 \right] \times \sigma_{\psi N}^{abs} \\ &\simeq 1.47 \times \sigma_{\psi N}^{abs} = 5.5 \text{ mb}, \end{aligned} \quad (25)$$

where the value $\sigma_{\psi N}^{abs} = 3.8 \text{ mb}$ has been used, according to our calculation in the previous section. We can therefore summarize saying that, although the cross section for Ψ with a singlet nucleon is 3.8 mb, including formation time effects, its effective value in AB collisions with large nuclei is 5.5 mb.

As a final remark, notice that the calculation leading to eqs. (21), (22), (23) and (24) is performed assuming that each projectile nucleon undergoes collisions with singlet nucleons in the target. This neglects the color excitation of the target. A complete treatment of the problem is very involved and is not expected to change the picture drawn. In fact, as seen in FIG. 5, color excitation is a rather fast process and accounting for the neglected features would make it even faster. Moreover, as discussed in the introduction, gluon radiation, here neglected, would speed up color excitation even more.

2 Charmonium Suppression in AB collisions

Having discussed in detail colored cross section and multiple color exchange, we obtained, with eq. (24), the important ingredient needed to calculate in detail the Ψ production cross section in AB collisions. It is first of all necessary to discuss some kinematical features concerning Ψ absorption and follow the longitudinal space-time diagram of FIG. 6, where the kinematics is illustrated. Considering the absorption caused by one of the nucleons of nucleus B , with coordinate z'_B , one notices that, before interacting with the meson at point D_B , it has traveled through nucleus A from $+\infty$ down to \tilde{z}_A . The position \tilde{z}_A depends on the Ψ velocity in the center of mass frame. This, in turn, depends on $x_F = 0.15$, from which one obtains that $v_\Psi = \sqrt{x_F^2 s / (4m_\Psi^2 + x_F^2 s)}$, where s is the center of mass

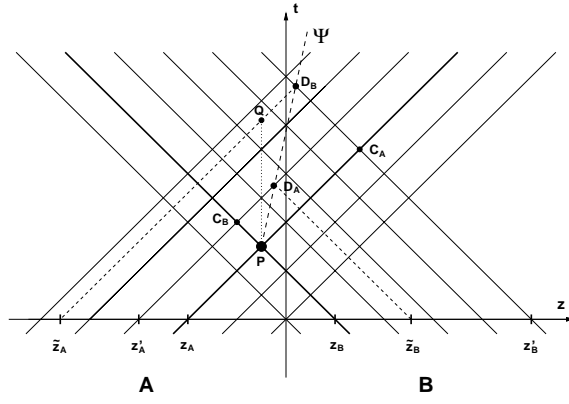


Figure 6: Longitudinal space-time representation of a row on row collision taking place at impact parameters (\vec{b}_A, \vec{b}_B) within a AB collision. The Ψ production point is indicated with P, while the absorption points by D_A and D_B , do to nucleons of A and B respectively.

energy of a NN collisions. With an elementary geometrical reasoning, making use of the triangle PQD_B for nucleus B , and $D_A C_B P$ for nucleus A , one arrives at the relations

$$\tilde{z}_A = z_A - (z'_B - z_B) R_\Psi, \quad \tilde{z}_B = z_B - (z'_A - z_A) R_\Psi^{-1}, \quad (26)$$

where $R_\Psi = (1 - v_\Psi)/(1 + v_\Psi)$. These must be used as arguments for the effective cross section in eq. (24). Therefore one has two cross sections, one for absorption by nucleus A , taking into account the multiple scattering of its nucleons with nucleus B , and one for nucleus B , depending on A . We can now modify eq. (16) by making the replacements

$$\sigma_{\Psi N}^{abs} T_A(z_A, \vec{b}_A) \rightarrow \int_{-\infty}^{z_A} dz'_A \Sigma_B(\tilde{z}_B, \vec{b}_B) \rho_A(z'_A, \vec{b}_A), \quad (27)$$

$$\sigma_{\Psi N}^{abs} T_B(z_B, \vec{b}_B) \rightarrow \int_{z_B}^{+\infty} dz'_B \Sigma_A(\tilde{z}_A, \vec{b}_A) \rho_B(z'_B, \vec{b}_B). \quad (28)$$

The position-dependent effective cross sections

$$\Sigma_A(\tilde{z}_A, \vec{b}_A) = \sum_n \sigma_{\Psi N_n}^{abs} P_n^A(\tilde{z}_A, \vec{b}_A), \quad (29)$$

$$\Sigma_B(\tilde{z}_B, \vec{b}_B) = \sum_n \sigma_{\Psi N_n}^{abs} P_n^B(\tilde{z}_B, \vec{b}_B), \quad (30)$$

are obtained from eq. (24).

Now eq. (16) can be used to evaluate total cross sections, with a further integration in impact parameter. We compute values to compare with all available data measured by the NA38/50/51

collaboration at the SPS [32]. We use realistic nuclear profiles [20] and scale the center of mass energy according to the parameterization $\sigma_{\Psi}^{NN} \sim (1 - m_{J/\psi}/\sqrt{s})^{12}$. The results are compared with the data in FIG. 7. The dashed curve corresponds to a standard Glauber model calculation with the singlet absorption cross section $\sigma_{\Psi N_1}^{abs} = 3.8$ mb, as evaluated in Sect. 3, while the thick curve refers to the improved calculation which takes into account color excitations, studied in Sect. 4. In order to emphasize the difference between the two absorption mechanisms, we neglect here anti-shadowing effects. For the pA calculation we increased the value of $\sigma_{\Psi N_1}^{abs}$ by 35 %, therefore used $\sigma_{\Psi N_8}^{abs} = 5.1$ mb. This is the extreme situation, when Ψ always encounters color octet nucleons. For the AB case we used eqs. (29) and (30). Since our main intent is to compare the the new absorption mechanism to the conventional Glauber model one, we do not present the calculation of the E_{\perp} -dependent cross section for Pb+Pb collisions, which we cannot explain.

Different from the Glauber model result, our improved one provides a better agreement with the data, except for the Pb+Pb point. In other words, the proposed absorption mechanism due to color dynamics is found to be an important contribution to nuclear effects in Ψ production. It must be accounted for, together with other mechanisms of suppression [15, 16, 33] which we here put aside. In the search for new physics one must in fact rely on a solid baseline, employing the best of our knowledge of the dynamics of Ψ absorption at the early stage of a nuclear collision.

5 Conclusions

In this work we studied the dynamics underlying Ψ suppression due to nuclear effects, employing the idea that color exchange processes in multiple NN collisions may play a significant role.

First of all, we calculated inelastic cross sections for Ψ scattering on colored nucleons and found an increase of about 35 % when the nucleon is in a color octet state as compared with the singlet case, while the enhancement factor for the color decuplet is about 70 %.

Making use of available calculations of ΨN cross sections, we included formation time effects and obtained the effective value for Ψ absorption on singlet nucleons $\sigma_{\Psi N_1}^{abs} = 3.8$ mb. Scaling this value with a 35 % increase we obtained $\sigma_{\Psi N_8}^{abs} = 5.1$ mb and with a 70 % increase $\sigma_{\Psi N_{10}}^{abs} = 6.4$ mb.

We then performed a fit to available data on Ψ production cross sections in pA collisions. The result

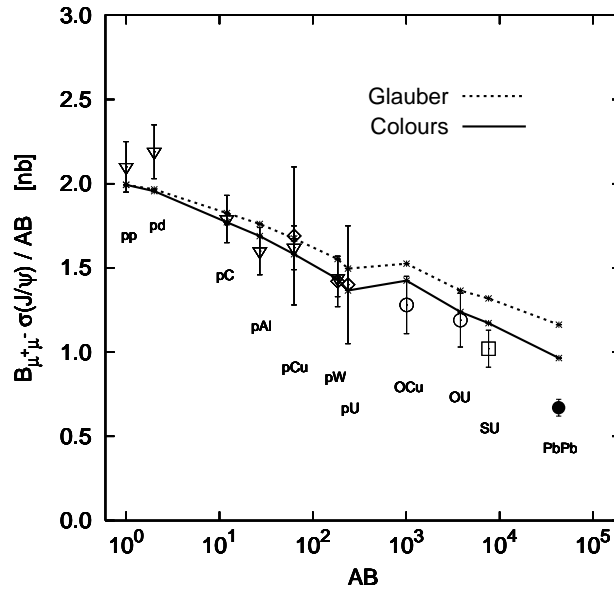


Figure 7: Calculations of total J/ψ production cross sections in AB collisions and comparison with the NA38/50/51 data. The curves, drawn to guide the eye, correspond to Glauber absorption (dashed) and to absorption by colored nucleons (full).

of the fit, including gluon anti-shadowing corrections, is that the effective absorption cross section for Ψ is $\sigma_{\Psi N}^{eff} = 5.7 \pm 0.6$ mb, therefore suggesting that in pA collisions, the produced charmonium interacts with color octet nucleons. The conclusion is, though, rather weak because the experimental points are quite scattered.

Total production cross sections for Ψ were then calculated and compared in FIG. 7 with available data for AB collisions. Compared to the Glauber model result, the agreement is improved and we conclude that effects due to color exchange processes are substantial and provide the value $\sigma_{\Psi N}^{abs} = 5.5$ mb for the effective absorption cross section on nucleons in AB collisions (See eqs. (24) and (25)).

In conclusion, we have completed a study of nuclear effects in charmonium production in AB collisions, providing a better baseline for future calculations. These amount to an improved treatment of gluon bremsstrahlung, including non-linearities arising because of gluon cascades, to the calculation of effects caused by gluon energy loss and to the evaluation of E_{\perp} -dependent cross sections. This will hopefully provide the starting point from which to address more precisely the nature of anomalous suppression in Pb+Pb collisions.

Acknowledgments

This work has been supported in part by the B.M.B.F. under contract number 06 HD 642.

References

- [1] C. Gerschel and J. Hüfner, Annu. Rev. Nucl. Part. Sci. **49** (1999) 255;
- [2] R. Vogt, Phys. Rept. **310** (1999) 197;
- [3] B. Z. Kopeliovich and B. G. Zakharov, Phys. Rev. **D44** (1991) 3466;
- [4] J. Hüfner, B. Z. Kopeliovich and J. Nemchik, Phys. Lett. **B383** (1996) 362;
- [5] J. Hüfner and B. Z. Kopeliovich, Phys. Rev. Lett. **76** (1996) 192;
- [6] J. Hüfner, B. Z. Kopeliovich and A. B. Zamolodchikov, Z. Phys. **A357** (1997) 113;
- [7] K. Ackerstaff *et al.* (HERMES Coll.), Phys. Rev. Lett. **82** (1999) 3025;
- [8] Y. B. He, J. Hüfner and B. Z. Kopeliovich, Phys. Lett. **B477** (2000) 93;
- [9] T. Matsui and H. Satz, Phys. Lett. **B178** (1986) 416;
- [10] J. Blaizot and J. Ollitrault, Phys. Rev. Lett. **77** (1996) 1703;
- [11] D. Kharzeev, C. Lourenco, M. Nardi and H. Satz, Z. Phys. **C74** (1997) 307;
- [12] S. Gavin and R. Vogt, Phys. Rev. Lett. **78** (1997) 1006;
- [13] N. Armesto and A. Capella, Phys. Lett. **B430** (1998) 23;
- [14] N. Armesto, A. Capella and E. G. Ferreira, Phys. Rev. **C59** (1999) 395;
- [15] J. Hüfner and B. Z. Kopeliovich, Phys. Lett. **B445** (1998) 223;
- [16] J. Hüfner, Y. B. He and B. Z. Kopeliovich, Eur. Phys. J. **A7** (2000) 239;
- [17] F. Low, Phys. Rev **D12** (1975) 163; S. Nussinov, Phys. Rev. Lett **34** (1975) 1286;

- [18] J. F. Gunion and D. Soper, Phys. Rev **D15** (1977) 2617;
- [19] J. Hüfner, Y. P. Ivanov, B. Z. Kopeliovich and A. V. Tarasov, Phys. Rev. **D62** (2000) 094022;
- [20] C. W. De Jager, H. De Vries and C. De Vries, Atom. Data Nucl. Data Tabl. **36** (1987) 495;
- [21] J. Badier *et al.* (NA3 Coll.), Z. Phys. **C20** (1983) 101;
- [22] M. C. Abreu, *et al.* (NA38 Coll.), Phys. Lett. **B 444** (1998) 516; M. C. Abreu, *et al.* (NA51 Coll.), Phys. Lett. **B 428** (1998) 35;
- [23] M. J. Leitch *et al.* (E866 Coll.), Phys. Rev. Lett. **84** (2000) 3256;
- [24] T. Gousset and H. J. Pirner, Phys. Lett. **B375** (1996) 349;
- [25] L. Frankfurt and M. Strikman, Eur. Phys. J. **A5** (1999) 293;
- [26] K. J. Eskola, V. J. Kolhinen and C. A. Salgado, Eur. Phys. J. **C9** (1999) 61;
- [27] B. Z. Kopeliovich and F. Niedermayer, *Nuclear Screening in J/ψ and Lepton Pair Production*, JINR-E2-84-834;
- [28] M. B. Johnson *et al.* (E772 Coll.), hep-ex/0010051.
- [29] B. Z. Kopeliovich and A. B. Zamolodchikov, unpublished, see in B. Z. Kopeliovich and L. I. Lapidus, *Colour Exchange of High Energy Hadrons in Nuclei*, Proc. of the VI Balaton Conf. on Nucl. Phys., p.103, Balatonfüred, Hungary, 1983;
- [30] V. N. Gribov, Sov. Phys. JETP **29** (1969) 483;
- [31] P. V. Ramana Murthy, C. A. Ayre, H. R. Gustafson, L. W. Jones and M. J. Longo, Nucl. Phys. **B92** (1975) 269;
- [32] M. C. Abreu, *et al.* (NA50 Coll.), Phys. Lett. **B 410** (1997) 337;
- [33] J. Hüfner, B. Z. Kopeliovich and A. Polleri, work in progress;